Problems of Tribology, V. 30, No 1/115-2025, 12-22

Problems of Tribology
Website: http://tribology.khnu.km.ua/index.php/ProbTrib
E-mail: tribosenator@gmail.com

DOI: https://doi.org/10.31891/2079-1372-2025-115-1-12-22

Analysis of damage to ceramic balls in hybrid rolling friction pairs

R. E. Kostunik[1], A. L. Maystrenko[2]*, A. S. Vasylchuk[2], D.S. Kustovskyi[2]

[1]Kyiv Aviation Institute, Kyiv, Ukraine
[2]V.M. Bakul Institute of Superhard Materials, National Academy of Sciences of Ukraine
**E-mail: almaystrenko46@gmail.com*

Received: 25 November 2024: Revised: 25 December 2024: Accept: 15 January 2025

Abstract

Most bearings are currently made primarily from steel, but they fail relatively quickly under high loads, temperatures, as well as abrasive, corrosive, chemical and other types of wear. Replacing steel balls with ceramic balls, i.e. creating hybrid bearings, in many cases allows achieving significantly higher performance and expanding the range of functionality of the devices in which they are used. For example, hybrid ball bearings take advantage of ceramic rolling elements with high quality surface treatment of steel rings, which allows for longer service life and better performance at high rotational speeds. As practice shows, hot-pressed silicon nitride (Si_3N_4) is the main material used to create hybrid bearings with ceramic rolling elements, although there is also interest in materials such as boron carbide (B_4C), silicon carbide (SiC) and aluminium oxide (Al_2O_3). However, there are no publications devoted to the analysis of the causes of formation and accumulation of damage to ceramic balls in hybrid rolling friction pairs. Therefore, the aim of the study is to determine the mechanism of formation and development of surface damage in ceramic balls of hybrid rolling friction pairs. As a result of the study, a technological cycle of electric sintering of ceramic ball blanks from Si_3N_4 under high pressure up to 4 GPa was created, which made it possible to compact the monophasic ceramic material to a practically poreless state. The technology of precision diamond processing of ceramic balls with a diameter of 12.7 mm is described.The paper presents the results of tribological tests of a hybrid rolling friction pair "Si_3N_4 ceramic balls - steel SHKH-15". For the first time, the mechanism of damage to the surface layers of ceramic balls in the form of the formation of surface fatigue microcracks, which lead to the formation of pitting and delamination of the surface layer, was investigated. For the first time, Walner lines were found on the pitting surfaces, which proves the fatigue mechanism of their formation and development.

Keywords: Electric sintering of ceramics, silicon nitride, diamond processing of ceramic balls, hybrid ball bearing, fatigue cracks, rolling friction, wear, pitting.

Indroduction

Most bearings are currently made primarily of steel, but they fail relatively quickly under high loads, temperatures, as well as abrasive, corrosive, chemical and other types of wear. Replacing steel balls with ceramic balls, i.e. creating hybrid bearings, in many cases allows achieving significantly higher performance and expanding the range of functionality of the devices in which they are used [1-3]. For example, hybrid ball bearings take advantage of the advantages of ceramic rolling elements with high quality surface treatment of steel rings, which allows for longer service life and better performance at high rotational speeds. As practice shows, hot-pressed silicon nitride (Si_3N_4) is the main material used to create hybrid bearings with ceramic rolling elements, although there is also interest in materials such as boron carbide (B_4C), silicon carbide (SiC) and aluminium oxide (Al_2O_3). A number of well-known companies manufacture and operate ceramic or hybrid rolling bearings [1-3]. However, there are no publications devoted to the analysis of the causes of formation and accumulation of damage to ceramic balls in hybrid rolling friction pairs. Therefore, the aim of the study is to determine the mechanism of formation and development of surface damage in ceramic balls of hybrid rolling friction pairs.

Sintering of ceramic materials under high pressure.

The hybrid rolling friction pair under study consists of ceramic balls made of Si3N4 and steel rings (counterbodies) made of bearing steel SHKH-15 [4] (analogue of AISI 52100). For wear-resistant ceramic

elements based on silicon nitride in hybrid ball bearings, one of the important requirements is high ceramic density, which is possible only in the absence of residual porosity, so hot pressing, hot isostatic pressing, as well as SPS and its modifications are used for their sintering [5,6]. A number of effective methods have been developed in the field of electric discharge sintering: the SPS (Spark Plasma Sintering) method and its analogue FAST (Field Assisted Sintering Technology), as well as EDS (Electric Discharge Compaction). The rapid heating of the powder briquette is realised by means of a high-frequency pulse discharge and the resulting plasma effect in the spark discharge. The main disadvantages are the relatively low pressing pressure of 100-500 MPa [6,7] and the uneven distribution of electric current in the sintered briquette. In addition, the level of applied pressure during hot pressing in graphite moulds is limited due to the relatively low strength and plastic deformation of graphite components at high temperatures. Typically, the billet is heated during sintering by induction heating of a graphite mould or by passing an electric current through the graphite components of the mould, as well as by resistive heating by passing an electric current of industrial frequency directly through the billet [8-10].

Electric sintering of ceramics under high pressure, which was implemented using the well-known principle of resistive heating of the briquette, but at a much higher pressure [8-10]. As a result of the high pressure and short duration of the sintering process, grain size growth is practically not observed. Due to the fact that ceramic balls made of silicon nitride are loaded in bearings under high contact stresses, we need to obtain a sintered porous billet with a density close to the theoretical one. These conditions can be met by using the process of resistive electro-sintering of ceramic material at high pressure (ESR) [10]. At the Bakul Institute of Materials Science, a high-pressure apparatus for the spontaneous synthesis of superhard materials and electric sintering of ceramic products was developed [9,11], which makes it possible to sinter conductive and non-conductive powder compositions at high pressures (4-8 GPa). In this setup, the sample is pre-pressed into a container made of lithographic stone, loaded with pressure, and an electric current is passed through the sample. The design of the unit allows for the consolidation of ceramic materials at pressures up to 4-5 GPa and temperatures up to 2000^0C [9,11]. The proposed method is relatively cheap and simple compared to other alternative existing technologies.

For the manufacture of ceramic balls, silicon nitride powder was used, which was obtained by the method of spontaneously combustion synthesis (SCS). The average size of the initial powder was <D>=4.8 μm, and the phase composition was Si3N4 1160 - 89%, Si_3N_4 0360 - 9%, SiO2 - 2%.

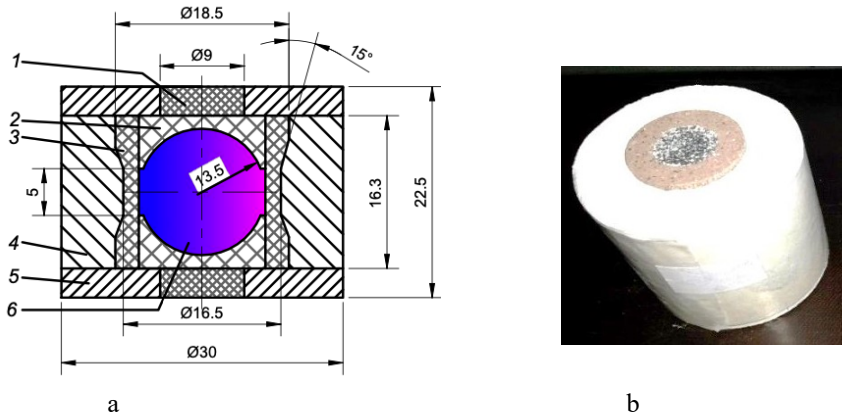

a b

Fig. 1. Schematic of the layout of the reaction vessel for sintering ceramic ball blanks in a high-pressure apparatus: 1 - graphite disc; 2 - graphite moulder; 3 - heater with TRG; 4,5 - container of silicate (pyrophyllite Al2[Si_4O_{10}] $(OH)_2$); 6 - ball blank from Si_3N4 powder; - (a); general view of the assembled container for sintering ceramic ball blanks from silicon nitride - (b)

For sintering ceramic ball blanks with a diameter of 12.7 mm, a high-pressure apparatus [11] based on a hydraulic press mod. DO-043 with a force of 20 MN and an electronic control system (software unit) for the sintering process.

Fig. 2. General view of sintered ceramic ball blanks

The materials and dimensions of the components of the reaction cell were preliminarily calculated in order to obtain a temperature distribution during billet sintering with a minimum temperature gradient along the diameter [9]. The layout of the reaction vessel for sintering ceramic ball blanks under high pressure is shown in Fig. 1,a. Cold pressing of ceramic ball briquettes was performed in steel moulds under a pressure of 180-200 MPa. After cold briquette pressing, the billets had a diameter of 15.4 mm and a total height of 19 mm. The compressed briquettes were placed in a container of a high-pressure apparatus. The sintering temperature of the billets was 1650^0C, the pressure was 4 GPa, and the duration was τ = 4 min. After sintering, the diameter of the billets was reduced to 13.5 mm and their height to 13.44 mm (Fig. 2).

All sintered billets were tested, as a result of which the average values of the ceramic material density, elastic and shear moduli, Poisson's ratio and Vickers hardness (HV) were determined on the basis of a sample of 30 samples - (Table 1).

Table 1

Physical and mechanical properties of Si_3N_4 ceramic balls (ESWT) and steel SHKH-15 used in the study of wear of a hybrid rolling friction pair

Characteristics	Steel SHKH -15 [4] (AISI 52100) [12,13]	Si_3N_4 (ESWT) [14]
Density, g/cm^3 (10^{-3}m)	7.812	3.187
Elastic modulus E, GPa	211	289
Shear modulus G, GPa	80	119
Poisson's ratio	0.28	0.26
Critical stress intensity factor K_{1c}, MPa.м$^{1/2}$	15.4–18.7	5.0
HV hardness at 20 °C	-	27.4

Manufacturing precision ceramic balls by diamond processing

Samples of precision ceramic balls were made from sintered Si_3N_4 billets (ESWT). At the preliminary stage, the workpieces were ground according to the scheme between two discs, one of which (upper) is a diamond wheel, and on the plane of the second (lower), located eccentrically, freely rotating balls had a circular feed. At the next stage, the precision balls were ground between two discs in a V-shaped annular groove in several stages with a consistent decrease in the diamond slurry grain size from ASM 28/20 to ASM 1/0 [17]. Thus, the test samples of balls with a diameter of 12.7 mm had a deviation from the spherical shape of 0.4 μm and a surface roughness of Ra 0.025 (accuracy class G16 according to ISO 3290-2:2014) [17,18] - Fig. 3.

Evaluation of the surface texture and condition of the near-surface layer of Si3N4 ceramic balls after diamond processing

The amplitude parameters Sa, Sq, Sp, Sv, St, Ssk, Sku were chosen to quantify the surface roughness of ceramic balls [18]. The surface topography of the balls was recorded using a non-contact interference 3D profilograph "Micron-alpha" based on an optical microscope II-4 by processing a sequence of interference patterns. The measurement area was 250 × 190 μm. The measurements were repeated 3-5 times in different areas. The calculation of roughness parameters was performed in the software environment "3D Surface Texture Mountains Map". The average values of the amplitude parameters of the surface roughness of Si_3N_4 ceramic balls are given in Table 2.

Table 2

Amplitude parameters of the surface roughness of a Si_3N_4 ceramic ball (ESWT) with a diameter of 12.7 mm after diamond processing

Sa ,mkm	Sq ,mkm	Sp ,mkm	Sv ,mkm	St ,mkm	Ssk	Sku	Sz ,mkm
0.0379	0.0572	0.2827	0.2712	0.5292	0.361	8.5975	0.4787

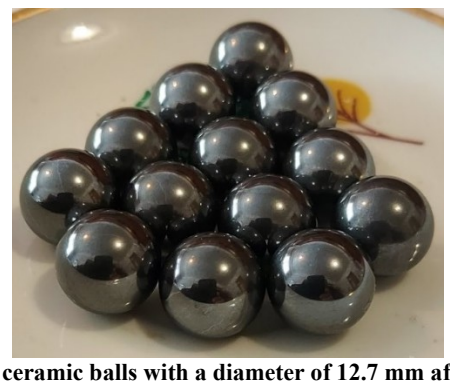

Fig. 3. General view of ceramic balls with a diameter of 12.7 mm after diamond processing

The manufactured balls were also cut along their diametrical cross-section to analyse the presence of microcracks in the surface layers after diamond processing, which was necessary to determine the subsequent evolution of damage as a result of the operation of the hybrid rolling friction pair. Examination of the near-surface layer of the ball's diameter cross-section using a Carl ZEISS EVO 50 XVP scanning electron microscope showed the absence of microcracks in the near-surface layer of the ceramic ball.

Tribological tests of ceramic balls for wear in a hybrid rolling friction pair

In order to determine the wear resistance of balls in the Si_3N_4 ceramic - SHKH-15 steel system under lubrication with an oil-vapour-gas mixture (TC-1 and MC-8p oil), a rapid test method was developed taking into account the geometric and kinematic parameters of the test assembly on the laboratory device for unidirectional three-point rolling friction KIIGA-1m (Fig. 4) [19,24].

The test assembly of the device simulates the geometry of the contact of rolling friction of balls on a steel support (Fig. 4), which allows simulating the friction processes of a real tribosystem of a deep groove ball bearing. The balls were centred using the standard raceway of the steel bearing ring, and the upper ring was mounted with a flat working surface.

For a comparative assessment of the wear resistance of the model thrust ball bearing and testing of the test methodology, serial balls of ball bearing 8211 (steel SHKH-15 (AISI 52100)) with a diameter of 12.7 mm not lower than the fourth degree of accuracy and prototypes of ceramic balls made of silicon nitride with a diameter of 12.7 mm were used. The initial friction conditions were determined by preliminary tests of serial steel and ceramic balls, namely: engine spindle speed - 1500 rpm; total maximum test time excluding periodic stops (every 15 minutes) to control the wear of the sample material; axial load under dry friction and in lubricant - 490 N; wear criterion for the steel sample - depth of the raceway; wear criterion for the test balls - loss of ball material weight.

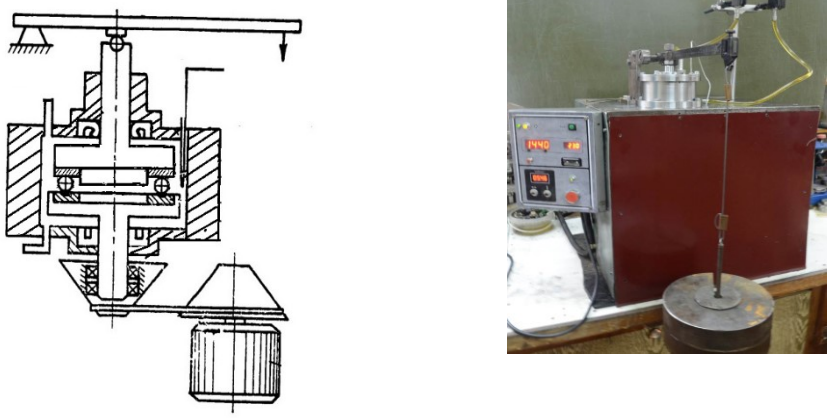

a b

Fig. 4. Scheme of testing a hybrid rolling friction pair [19] - (a); General view of the setup for tribological testing of ceramic balls - (b)

A stationary thrust ball bearing ring 8211 made of steel SHKH -15 was mounted on the holder, with the standard raceway facing outwards. At the bottom of the chamber, namely on its lower surface, a movable sample (lower thrust ball bearing ring, steel SHKH -15) was mounted up the previously finished working surface, on which a separator with test ball samples was installed.After that, the separator was centred relative to the centre of rotation by positioning the balls in accordance with the raceway of the standard ball bearing ring pre-installed on the holder's seating surface. The chamber was filled with lubricant, and the necessary calibrated weights were placed on the lever of the loading system.The total time for the tribological tests was up to 6 hours. The wear rate of the lower steel ring was based on the linear wear of the ball bearing working surface and the weight loss of the test balls measured by profiling.

Determination of the contact pressure in the contact zone between the ball and the steel base

It is known that the wear rate of the friction pair components depends not only on the kinematic operating conditions of the rolling friction unit, but also on the level of contact pressure. For this purpose, the level of contact stresses in the contact area of a ceramic ball with a steel ring groove was estimated (Fig. 5). A ball of radius is located in a cylindrical groove (trough) with radius r > R under a load P = 490 N:

$$\frac{1}{R_1} = \frac{1}{R} - \frac{1}{r}, \quad \frac{1}{R_2} = \frac{1}{R}.$$

The X-axis is directed perpendicular to the cylinder face. Due to the fact that the ball is in contact with the surface of the counterbody on a cylindrical surface rather than a plane, the contact patch is elliptical. The line of action of the compressive force is P normal to the elliptical area of the contact patch and passes through its centre.

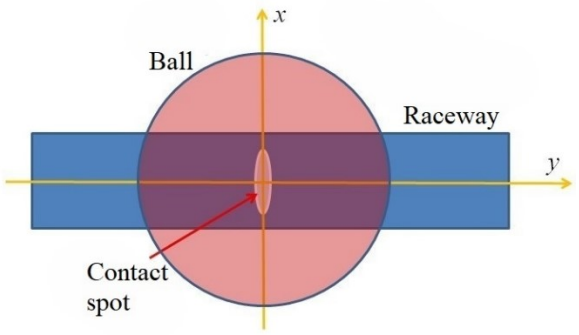

Fig. 5. Diagram of the formation of a contact spot of a ceramic ball on the surface of a groove in a steel support ring

The eccentricity $e=\sqrt{1-(b/a)^2}$ of the elliptical contact patch with the a>b axes is the solution of the transcendental equation [20]

$$\frac{R_2}{R_1}=\frac{\left(1-e^2\right)\left[\mathrm{K}(e)-\mathrm{E}(e)\right]}{\mathrm{E}(e)-\left(1-e^2\right)\mathrm{K}(e)},$$

where $\mathrm{K}(e)$ and $\mathrm{E}(e)$ are complete elliptic integrals of the first and second kind, respectively. A more convenient transcendental equation for analysis with respect to χ = a / b is:

$$\chi_{n+1}=\left[\frac{R_1}{R_2}\frac{R_D\left(0,\chi_n^{-3/2},\chi_n^{1/2}\right)}{R_D\left(0,\chi_n^{3/2},\chi_n^{-1/2}\right)}\right]^{2/3},$$

where $\mathrm{R}_D(p,q,r)=\frac{3}{2}\int_0^\infty \frac{\mathrm{d}t}{\left[(t+p)(t+q)(t+r)^3\right]^{1/2}}$

is the elliptic Carlson integral of the second kind [21]. It is solved by the iteration method [22] with the initial approximation:

$$\chi_0=\left(\frac{R_1}{R_2}\right)^{2/3}.$$

The semi-axes of the ellipse:

$$a=\left[\frac{PR_1}{\pi E^*}R_D\left(0,(b/a)^2,1\right)\right]^{1/3},\quad b=\left[\frac{PR_2}{\pi E^*}R_D\left(0,(a/b)^2,1\right)\right]^{1/3},$$

where $E^*=\left(\frac{1-\nu_1^2}{E_1}+\frac{1-\nu_2^2}{E_2}\right).$

Pressure distribution over the contact patch:

$$p=\frac{3P}{2\pi ab}\sqrt{1-\frac{x^2}{a^2}-\frac{y^2}{b^2}}.$$

Pressure in the centre of the spot:

$$p_0=\frac{3}{2}p_m=\frac{3}{2}\frac{P}{\pi ab},$$

where p_m is the average pressure.

In the contact area along the axis along the axis $x\ (y=0)$:

$$\frac{\sigma_x}{p_0}=-2\nu\gamma-(1-2\nu)\frac{b}{ae^2}\left[\left(1-\frac{b\gamma}{a}\right)-\frac{x}{ae}\operatorname{arth}\left(\frac{ex}{a+b\gamma}\right)\right],$$

$$\frac{\sigma_y}{p_0}=-2\nu\gamma-(1-2\nu)\frac{b}{ae^2}\left[\left(\frac{a\gamma}{b}-1\right)+\frac{x}{ae}\operatorname{arth}\left(\frac{ex}{a+b\gamma}\right)\right],$$

where $\gamma=\sqrt{1-x^2/a^2-y^2/b^2}$ i $\operatorname{arth}(x)=\frac{1}{2}\ln\left(\frac{1+x}{1-x}\right)$ is the hyperbolic arctangent.

In the centre of the spot we have [23]

$$\frac{\sigma_x}{p_0}=-2\nu-(1-2\nu)\frac{b}{a+b},\quad \frac{\sigma_y}{p_0}=-2\nu-(1-2\nu)\frac{a}{a+b},\quad \frac{\sigma_y}{p_0}=-1.$$

Outside the contact spot, we have only shear stress:

$$\frac{\sigma_x}{p_0} = -2\nu\gamma - (1-2\nu)\frac{b}{ae^2}\left[\left(1-\frac{b\gamma}{a}\right) - \frac{y}{ae}\operatorname{arctg}\left(\frac{aey}{b(a\gamma+b)}\right)\right],$$

$$\frac{\sigma_y}{p_0} = -2\nu\gamma - (1-2\nu)\frac{b}{ae^2}\left[\left(\frac{a\gamma}{b}-1\right) + \frac{y}{ae}\operatorname{arctg}\left(\frac{aey}{b(a\gamma+b)}\right)\right],$$

$$\frac{\sigma_x}{p_0} = -\frac{\sigma_y}{p_0} = -(1-2\nu)\frac{b}{ae^2}\left[1-\frac{x}{ae}\operatorname{arth}\left(\frac{ex}{a}\right) - \frac{y}{ae}\operatorname{arctg}\left(\frac{aey}{b^2}\right)\right],$$

$$\frac{\tau_{xy}}{p_0} = -(1-2\nu)\frac{b}{ae^2}\left[\frac{y}{ae}\operatorname{arth}\left(\frac{ex}{a}\right) - \frac{x}{ae}\operatorname{arctg}\left(\frac{aey}{b^2}\right)\right].$$

Table 3

The size of the contact spot and stresses in its centre for groove radii in a steel ring r = 6.5405 mm and a ceramic ball R = 6.35 mm under a total load P = 490 N on 3 balls simultaneously (i.e. 163.3 N each)

r / R	a, mm (10^{-3} м)	b, mm (10^{-3} м)	S, mm^2 (10^{-6} $м^2$)	p_0, GPa
1.030	0.655	0.068	0.140	0.714

It is expected that close values of r and R correspond to a larger contact patch and, consequently, a lower stress level. Thus, the contact pressure in the center of the contact patch can reach 0.714 GPa, which is twice the contact fatigue limit for ceramics of this type [15].

Characterization of ceramic ball surfaces after tribological tests

Quantitative analysis of the parameters of the topography of the surfaces of ceramic balls after tribological tests was also carried out using a noncontact interference 3D profiler "Micron-alpha". The determined average values of the results of calculating the parameters of surface roughness of the spent ceramic balls made of Si_3N_4 are given in Table 4.

Table 4

Parameters of the surface condition of a ceramic ball Ø12.7 mm made of Si_3N_4 after tribological tests

Sa , mkm	Sq, mkm	Sp, mkm	Sv, mkm	St, mkm	Ssk	Sku	Sz, mkm
0.1176	0.1986	0.752	0.9276	1.68	0.2640	4.1740	1.4680

Table 4 shows that due to the friction of a ball in a hybrid rolling pair, damage is formed on its surface, resulting in an increase in its roughness by 3.1 times in the Sa parameter and by 3.37 times in the Sq parameter, which is confirmed by the damage observed in the near-surface layer of balls (Figs. 9-10).

Analysis of the results

Based on the tribological tests performed, the total mass loss of three ceramic and steel balls as a result of their wear when rolling on a steel ring was determined (Fig. 6) and the wear intensity of a flat steel ring (steel SHKH-15) was determined (Fig. 7) [24].

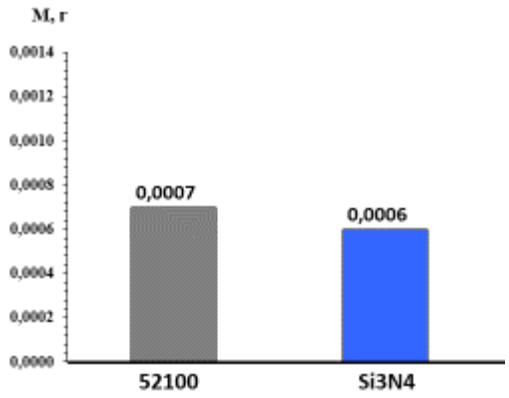

Fig. 6. Total mass loss of three balls made of Si3N4 ceramics and SHKH -15 steel under friction under conditions of lubrication with an oil-vapor-gas mixture

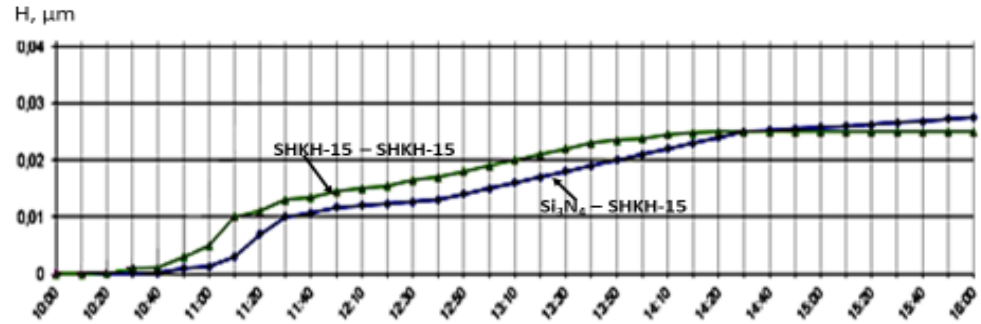

Fig. 7. Graph of wear intensity of a flat sample (steel SHKH-15) over time under rolling friction ceramic and steel balls in an oil-vapor-gas mixture

Analysis of the surface condition of ceramic balls after tribological tests

Pitting corrosion is accompanied by the formation of pits on the surfaces of the friction pair components, which start from the surface. This is a special case of fretting corrosion, which is formed during the cyclic mutual movement of two surfaces in contact. Contact fatigue includes two subcategories: subsurface and surface fatigue. The formation of subsurface fatigue cracks [25] is caused by the cyclic loading of the contacting surfaces, in fact, in the studied case, it is the local cyclic loading of a Ø12.7 mm ball with steel rings at a shaft rotation speed of 1500 rpm, i.e., 510.10^3 rpm/h. The number of cycles of contact loading is (at a cycle asymmetry factor of R=0), excluding slippage, 1020.10^3 contacts of the ball with the surfaces of the rings, which leads to a change in the material structure and leads to the formation of microcracks. Microcracks are formed in the near-surface layer, often in foreign inclusions in the material, and extend to the surface in the form of chips.

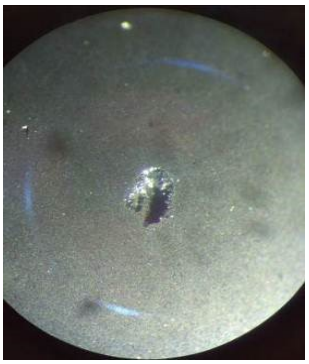

Fig. 8. General view of the pitting formed on the surface of a ceramic ball of Si_3N_4 with a diameter of 12.7 mm after 6 hours of loading in a hybrid rolling friction pair

The level of fatigue strength of ceramics of this type reaches the number of load cycles $\leq 10^7$ according to estimates in [15] 350-400 MPa and in [26] 300-450 MPa, which are 2-3 times lower than those in the studied rolling friction pair (see Table 3). That is, this leads to a high probability of the formation of localized cracks of contact fatigue, the signs of which are shown in Fig. 9.

Thus, during cyclic loading of ceramic balls in a hybrid rolling friction pair, as a result of contact fatigue, damage in the form of microcracks is formed and accumulated in the surface layer, which are oriented relative to the contacting surface at an angle of 250-300 (Fig. 9). Their further development leads to the formation of surface pits, i.e., pitting with distinct Wallner curves that reflect the process of fatigue crack propagation (Fig. 10 b, c), according to the kinetic diagram of fatigue crack propagation in Si_3N_4 ceramics [15].

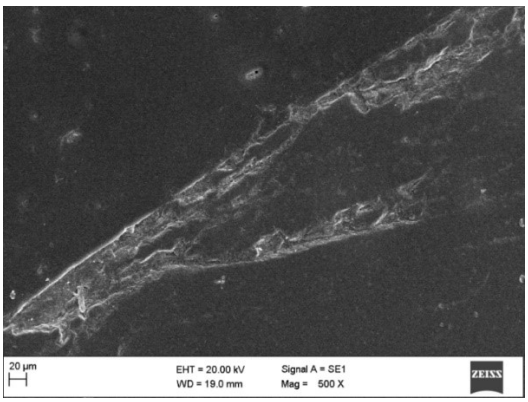

a

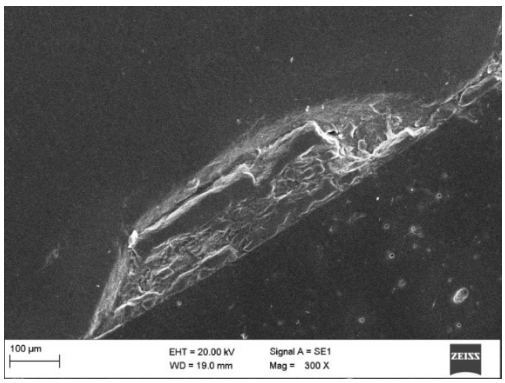

b

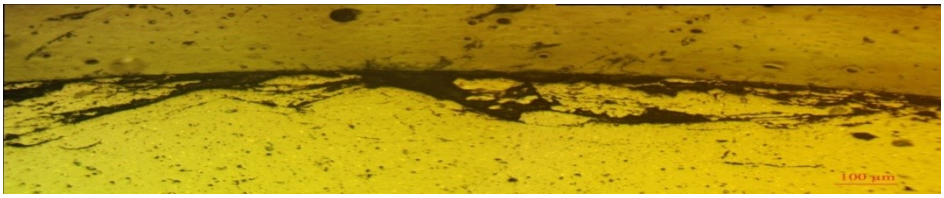

c

Fig. 9. Damage to the surface layer of the grinded section of a Si3N4 ceramic ball as a result of of contact fatigue in a hybrid rolling friction pair

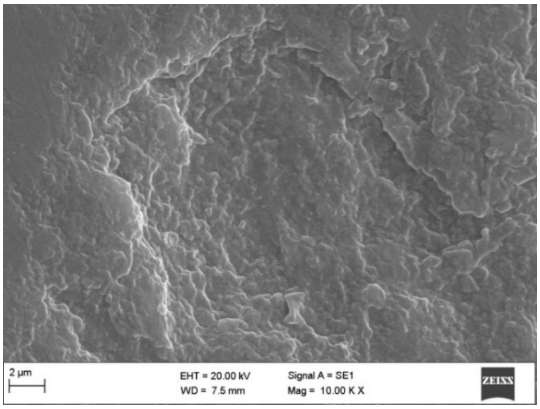

a

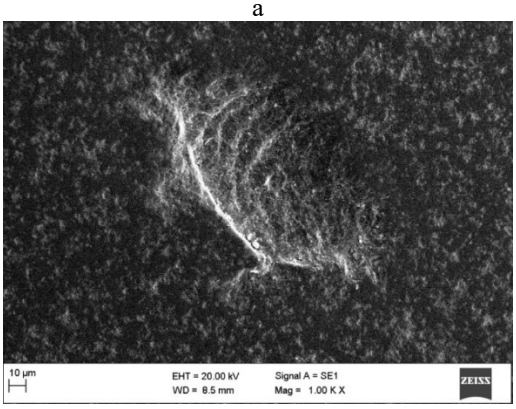

b

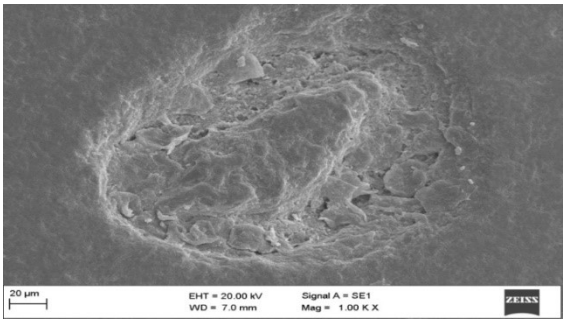

c

Fig. 10. Pitting on the surfaces of Si_3N_4 ceramic balls

A similar phenomenon of surface damage formation in the form of pitting is also observed on steel rails under the conditions of wheel rolling on the rail surface with a high probability of formation of such defects of contact-fatigue origin [27]. This paper theoretically determines the characteristic angle of formation and propagation of surface cracks in rail heads (10°-40°), which is the main factor in the formation of typical surface contact-fatigue damage such as pitting. The contact pressure of a stamp (ball or wheel model) on a half-plane is modelled by unidirectional repeated translational movement along the edge of the half-plane of the Hertzian contact forces with a tangential component.

Thus, comparing the values of K_{th} given in Table 5, it becomes clear why pitting occurs in a ceramic ball rather than in a steel ring, since the values of K_{th} for Si_3N_4 ceramics are almost 2 times lower than for steel SHKH -15 (Table 5).

Table 5

Comparative characteristics of the kinetic diagram of fatigue crack propagation in the materials of the studied rolling friction pair

Materials of friction pair	Density ρ, g/cm^3 (10^{-2} м)	Elastic modulus E, GPa	Threshold value of the intensity factor at the beginning of fatigue crack growth K_{th}, MPa.м$^{1/2}$	Critical stress intensity factor K_{Ic}, MPa.м$^{1/2}$
Si_3N_4 [14-16, 26,28]	3.187	289	2.5 - 3.0	5.0
Steel SHKH -15 [12,13]	7.812	211	5.0 - 6.0	15.4-18.7

Conclusions

For the first time, the possibility of sintering ceramic ball blanks from Si_3N_4 at a pressure of 4 GPa with a density close to the theoretical one was shown. The total mass loss of three Si3N4 ceramic balls during tribological tests based on 6 hours in an oil-vapour-gas mixture was 0.0006 mg.

It is shown that the formation and development of surface damage in ceramic balls of hybrid rolling friction pairs is determined by the level of acting contact cyclic stresses, which are the main factor influencing the formation and development of surface fatigue cracks.

For the first time, it is shown that damage to the surface layer of a ceramic ball made of silicon nitride is caused by contact fatigue during cyclic loading of the ball in the process of rolling along the annular groove of the steel counterbody of a hybrid bearing, in the form of delamination and crushing of the surface layer to a depth of 120-150 μm, resulting in the formation of pitting corrosion pits on the surface of ceramic balls. Moreover, pitting is formed in ceramic balls because the threshold value of the stress intensity factor at the beginning of fatigue crack growth K_{th} in ceramics is 2 times lower than in steel SHKH -15 .

References

1.Yoshikiyo Yukawa. Trends and Future Prospects for Rolling Bearing Technologies.
Koyo Engineering Journal . English Edition. 2001. No. 159E.

2. Gregory A. Zimmerman. The Sky is the Limit . SKF, Evolution. 2016.

3. Gloeckner P., Rodway C. The Evolution of Reliability and Efficiency of Aerospace Bearing Systems . Engineering. 2017. Vol. 9. - pp. 962–991.

4. GOST 801-78. “Ball-bearing steel. Technical conditions. Moscow. 1978

5. Kislyy, P. / Boron carbide (Kislyy, P. , Kuzenkova,M. , Bodnaruk, N. and Grabchuk, B. Kyiv: Naukova dumka, 1988. - 216 p. (in Russian)

6. Groza J./Sintering activation by external electrical field . Groza J., Zavaliangos A. Materials Science and Engineering A. – 2000. – 287, №2. – pp. 171–177.

7. Salvatore Grasso / Highly Transparent Pure Alumina Fabricated by High-Pressure Spark Plasma Sintering. Salvatore Grasso,Byung-Nam Kim, Chunfeng Hu, Giovanni Maizza, and Yoshio Sakka. J. Am. Ceram. Soc., 93 [9].- 2010.- pp. 2460–2462.

8. Patent Ukraine No. 2064367(RF). Installation for hot pressing of products from high resistive composite materials”, Pereyslov, V., Bologova, L., Kulich, L., Simkin, E., Maystrenko, A. 27.07.1996. - № 21.

9. V. A. Dutka / Modeling the Temperature Field in a High-Pressure Apparatus during the Sintering of Large-Sized Products Based on Boron Carbide. V. A. Dutka, A. L. Maystrenko, O. I. Borymskyi, V. G. Kulich and T. O. Kosenchuk . Journal of Superhard Materials. - 2020, Vol.42, No. 4. - pp. 240–250.

10. A. L. Maystrenko./ Electrosintering of ceramic materials . A. L. Maystrenko, O. I. Borymskyi ,V. G. Kulich, V. A. Dutka , D.O. Stratiychuk. Kyiv: Naukova dumka. – 2022. - 297 p. (in Ukraine).

11. N. V. Novikov /Steel high pressure apparatus for synthesis of superhard materials . N. V. Novikov, A. I. Prikhna, A. I. Borimsky. High Pressure Research and Industry VIII AIRAPT Conf., Upsala, Aug. 17–22, 1981. – Upsala, 1982. – 2. – pp. 790–792.

12. J.A. Rescalvo Santiago. Fracture and fatigue crack growth in 52100, m-50 and 18-4-1 bearing steels .Submitted in partial fulfillment of the requirements for the degree of doctor of philosophy. Massachusetts Institute of Technology. June 1979. -197 p.

13. Beswick J. M. Fracture and fatigue crack propagation properties of hardened 52100 steel. Metallurgical Transactions A, vol. 20, 1989. - pp. 1961–1973.

14. Maystrenko, A./ Treschinostoykost kristalicheskikh i kompozitcionikh sverkhtverdikh materialov. Novikov, N., Maystrenko, A., Physicochemical mechanics of materials (PCMM), 1983.-No4, pp. 46-53. (in russion)

15. Robert O. Ritchie / Cyclic Fatigue of Ceramics: A Fracture Mechanics Approach to Subcritical Crack Growth and Life Prediction . Robert O. Ritchie and Reinhold H. Dauskardt. Journal of The Ceramic Society of Japan . - 99 [10] . -1991. - pp.1047-1062.

16. Mehanika razrushenia I prochnost materialov, V.4. Ustalost i tciklicheskay reshinostoykoct konstruktcionikh materialov. Kyiv. Naukova dumka. 1990. (in russion)

17. Sokhan' S./ Diamond Grinding of Ceramic Balls with a Circular Feed. Voznyi V., Sorochenko V., Hamaniuk M., Journal of Superhard Material.-2023.-vol. 45, No 4. pp. 293–305.

18. ISO 3290-2:2014(en). Rolling bearings - Balls - Part 2: Ceramic balls https://www.iso.org/obp/ui/ru/#iso:std:iso:3290:-2:ed-2:v1:en

19. Aksenov A.F. Trenie I iznashivanie metalov v uglevodorodnikh jidkostyakh [Aksenov A.F. Friction and wear of metals in hydrocarbon liquids. - M.: Mashinostroenie] - 1977. – 152 c. (in russion)

20. Lurie A. I. Prostranstvennye zadachi teorii uprugosti [Spatial Problems of Theory of Elasticity]. Moscow, Gostekhizdat. -1955.(in russion)

21.Carlson B. C. Computing elliptic integrals by duplication. Numerische Mathematik, 33. - 1979. - pp.1-16.

22.Greenwood J. A. Hertz Theory and Carlson Elliptic Integrals . J. Mech. Phys. Solids, 119 (2018) - pp.240-249.

23.Johnson K. L. Contact Mechanics. Cambridge University Press, 1985.

24. A. L. Maystrenko / Rolling Friction of Hybrid Ceramic–Steel Pairs under Different Lubrication Conditions. A. U. Stelmakh, b, R. E. Kostunik, V. A. Radzievskiy , A. L. Maystrenko, S. V. Sokhan , V. G. Kulich . Journal of Friction and Wear. - 2020, Vol. 41, No. 5, pp. 432–442.

25. ISO 15243 Rolling bearings — Damage and failures — Terms, characteristics and causes Roulements — Détérioration et défaillance — Termes,caractéristiques et causes. – 2017.- Geneva, Switzerland

26. J.K. Tien / Fatigue and Creep Behavior of Si3N4 and SiC for Gas Turbine Applications. J.K. Tien, R. M. Arons , L. Roth. FP-1060 Research Project 271 Final Report, Prepared by Columbia University. Henry Krumb School of Mines Metallurgy Division New York, New York 10027 .- May 1979.

27. O. P. Datsyshyn / Pitting formation during fretting fatigue. O. P. Datsyshyn, O. S. Kalahan, V. M. Kadira, R. B. Shchur Physicochemical Mechanics of Materials. - 2004.-№2. - p.7-19.

28. Carrasquero-Rodríguez Edwuin / Determination of fracture toughness and elastic module in materials based silicon nitride /Carrasquero-Rodríguez Edwuin , Jaime Moisés , Romero-Romero Byron Ramiro , Luis Marcelo . Ingeniería Investigación y tecnología, vol. XX (núm.4), oct.-diciem. 2019: - pp.1-13. https://. orcid org/0000-0003-1047-398X

Костюник Р.Є., Майстренко А.Л., Васильчук О.С., Кустовский Д.С. Аналіз пошкоджень керамічних куль в гібридних парах тертя кочення

Вперше описаний технологічний цикл електроспікання керамічних заготовок куль з Si3N4 під високим тиском до 4 ГПа. Описана технологія прецизійної алмазної обробки керамічних куль діаметром 12.7 мм. В статті наведені результати трибологічних випробувань гібридної пари тертя кочення «керамічні кулі Si3N4 – сталь 52100». Вперше досліджено механізм пошкодження поверхневих шарів керамічних куль у вигляді формування поверхневих мікротріщин втоми, які приводять до утворення піттінга та відшарування приповерхневого шару. Вперше визначені лінії Вальнера на поверхнях утвореного піттінгу, що доводить втомний механізм їх утворення й розвитку.

Ключові слова: електроспікання кераміки при високому тиску, нітрид кремнію, алмазна обробка керамічних куль, гібридний шарикопідшипник, тертя кочення, зношування, піттінг